

Exploring the possible gluon condensation signature in gamma-ray emission from pulsars

Jianhong Ruan, Zechun Zheng and Wei Zhu*

Department of Physics, East China Normal University, Shanghai 200241, China

Abstract

The very high energy gamma-ray emissions from pulsars are usually considered to be dominated by leptonic scenario since the hadronic flux is weak. We point out that the gluon condensation predicted by a nonlinear QCD evolution equation may greatly enhance the cross sections of proton-target interactions and give rise to a characteristic broken power law in the gamma-ray spectra. The result is used to explore the gluon condensation signature in the observed gamma-ray spectra from pulsars.

keywords: Gluon condensation: Astroparticle physics: Gamma ray pulsars:

1 Introduction

Gluons are Bosons. Can gluons be stacked in a same quantum state like Bose-Einstein condensate (BEC)? How to observe this gluon condensation (GC) phenomenon? Gluons, confined in proton/neutron, are the fundamental components of the Universe. Previous works concerning the gluon distribution in proton based on QCD have shown the possible existence of GC [1-3]. The correlations among gluons at very high energy (VHE) may excite chaos in proton, which arises strong shadowing and antishadowing effects, resulting in the squeeze of gluons to a state with critical momentum. Accordingly, we found a series of likely GC signals in the VHE cosmic ray (gamma-ray, electron/positron, proton and nuclei) spectra, the sources include supernova remnants (SNRs), active galactic nuclei (AGN) and gamma ray bursts (GRBs) [4-7]. The present work focuses on the GC effect in gamma-ray spectra from pulsars.

*Corresponding author, E-mail:wzhu@phy.ecnu.edu.cn

Pulsars as rapidly rotating and magnetized neutron stars, can generate bubbles of relativistic particles when their ultra-relativistic winds interact with the surrounding medium, and the particles can be accelerated by pulsar wind nebulae (PWNe) up to PeV and beyond. It is widely accepted that the electromagnetic spectrum of pulsars originates from leptons. Although protons (or ions more generally) may exist in pulsars and further be accelerated, the hadronic scenario in pulsars is negligible since their fluxes are very weak in the pulsar surroundings [8]. However, the GC effect may largely increase the pp cross section by several orders of magnitude [3], which may compensate for the weak proton flux and produce the observed gamma rays. Therefore, we try to look for the GC signature in the gamma-rays from pulsars.

In section 2, we give a brief introduction of the GC model and present a complete VHE gamma-ray spectrum predicted by this model in figure 2, which shows the typical power law on both sides of the sharp turning point at E_{π}^{GC} . On the right side of this spectrum there is an exponential cutoff from $E > E_{\pi}^{cut}$.

In sections 3, we try to identify the GC-signature in the gamma-ray spectra of pulsars, and some examples are discussed. Due to the complex structure of the source, the recorded spectrum may come from different emission mechanisms, we will only focus on the part that related to the GC-spectrum.

Several VHE sources are tagged as unidentified and located near other bright ones. Although many works have speculated the possible origins of their spectra, the nature of them is still unknown. The simple GC-spectrum with a few free parameters allows us to infer the GC signals hidden in other mixed spectra. We give such examples in section 4. After the analysis of the above examples, the discussions and summary are presented in section 5.

2 The GC model

The flux of high energy gamma ray in hadronic processes $p + p \rightarrow \pi^0 \rightarrow 2\gamma$ in the laboratory frame reads [4-7]

$$\Phi_\gamma(E) = C_\gamma \left(\frac{E}{1\text{GeV}} \right)^{-\beta_\gamma} \int_{E_\pi^{\min}}^{E_\pi^{\max}} dE_\pi \left(\frac{E_p}{1\text{GeV}} \right)^{-\beta_p} \times N_\pi(E_p, E_\pi) \frac{d\omega_{\pi-\gamma}(E_\pi, E)}{dE}, \quad (2.1)$$

where the spectral index β_γ denotes the propagating loss of gamma-rays near the source. The accelerated protons obey a power law $N_p \sim E_p^{-\beta_p}$ with the index β_p . C_γ incorporates the kinematic factor with the flux dimension and percentage of $\pi^0 \rightarrow 2\gamma$. The normalized spectrum for $\pi^0 \rightarrow 2\gamma$ is

$$\frac{d\omega_{\pi-\gamma}(E_\pi, E)}{dE} = \frac{2}{\beta_\pi E_\pi} H\left[E; \frac{1}{2}E_\pi(1 - \beta_\pi), \frac{1}{2}E_\pi(1 + \beta_\pi)\right], \quad (2.2)$$

where $\beta_\pi \sim 1$, and $H(x; a, b) = 1$ ($a \leq x \leq b$) or $H(x; a, b) = 0$ (otherwise). Usually, the relations among N_π , E_π and E_p are very complicated and determined by using the limited experimental data. However, we show that the GC effect simplifies the above relations and gives a special energy spectrum. Since the more gluons, the more secondary pions in the inelastic pp collision, we assume that a huge number of gluons at the central region due to the GC effect may create the maximum number N_π of pions, which take up all available kinetic energy if we neglect the other secondary particles. One can get the following characteristic distributions in the GeV-unit

$$\ln N_\pi = 0.5 \ln E_p + a, \quad \ln N_\pi = \ln E_\pi + b, \quad (2.3)$$

$$\text{where } E_\pi \in [E_\pi^{GC}, E_\pi^{\max}],$$

and

$$a \equiv 0.5 \ln(2m_p) - \ln m_\pi + \ln K, \quad b \equiv \ln(2m_p) - 2 \ln m_\pi + \ln K, \quad (2.4)$$

$K \simeq 0.5$ is the inelasticity.

Substituting equations (2.2)-(2.4) into equation (2.1), we directly get the gamma ray spectrum,

$$E^2 \Phi_\gamma^{GC}(E) = \begin{cases} \frac{2e^b C_\gamma}{2\beta_p - 1} (E_\pi^{GC})^3 \left(\frac{E}{E_\pi^{GC}} \right)^{-\beta_\gamma + 2} & \text{if } E \leq E_\pi^{GC}, \\ \frac{2e^b C_\gamma}{2\beta_p - 1} (E_\pi^{GC})^3 \left(\frac{E}{E_\pi^{GC}} \right)^{-\beta_\gamma - 2\beta_p + 3} & \text{if } E > E_\pi^{GC}. \end{cases} \quad (2.5)$$

Surprisingly, it shows a typical broken power law.

Figure 1 is a schematic diagram for the gluon rapidity distribution with the GC effect at the pp collision, which is taken from [3]. One can find that the GC effect begins to work if it's peak locates at $y_{max} = \ln(\sqrt{s_{p-p}^{GC}}/\underline{k}_c)$, thus

$$x_c = \frac{\underline{k}_c}{\sqrt{s_{p-p}^{GC}}} e^{-y_{max}} \simeq \frac{\underline{k}_c^2}{s_{p-p}^{GC}}. \quad (2.6)$$

Applying $\sqrt{s_{p-p}} = \sqrt{2m_p E_p}$ into equation (2.3), one gets

$$E_\pi^{GC} = \exp \left(0.5 \ln \frac{\underline{k}_c^2}{2m_p x_c} - (b - a) \right). \quad (2.7)$$

On the other hand, the cross section of the pp collision disappears if the peak of gluon distribution moves to the rapidity center $y = 0$, i.e., at

$$x_c = \frac{\underline{k}_c}{\sqrt{s_{p-p}^{max}}} e^{y=0}, \quad (2.8)$$

or at

$$E_\pi^{max} = \exp \left(0.5 \ln \frac{\underline{k}_c^2}{2m_p x_c^2} - (b - a) \right) = \frac{E_\pi^{GC}}{\sqrt{x_c}}$$

$$= e^{b-a} \sqrt{\frac{2m_p}{k_c^2}} (E_\pi^{GC})^2 = 14(E_\pi^{GC})^2. \quad (2.9)$$

However, figure 1 shows that the plateau is shrinking as energy increasing rather than expanding, since lots of soft gluons enter the interaction range early due to the condensation, which implying that the suppression of Φ_γ occurs before E_π^{max} . Therefore we add a cut-off factor in equation (2.5), i.e.,

$$E^2 \Phi_\gamma^{GC}(E) = \begin{cases} \frac{2e^b C_\gamma}{2\beta_p - 1} (E_\pi^{GC})^3 \left(\frac{E}{E_\pi^{GC}}\right)^{-\beta_\gamma + 2} & \text{if } E \leq E_\pi^{GC}, \\ \frac{2e^b C_\gamma}{2\beta_p - 1} (E_\pi^{GC})^3 \left(\frac{E}{E_\pi^{GC}}\right)^{-\beta_\gamma - 2\beta_p + 3} & \text{if } E_\pi^{GC} < E < E_\pi^{cut}, \\ \frac{2e^b C_\gamma}{2\beta_p - 1} (E_\pi^{GC})^3 \left(\frac{E}{E_\pi^{GC}}\right)^{-\beta_\gamma - 2\beta_p + 3} \exp\left(-\frac{E}{E_\pi^{cut}} + 1\right) & \text{if } E \geq E_\pi^{cut}, \end{cases} \quad (2.10)$$

or

$$\Phi_\gamma^{GC}(E) \equiv \begin{cases} \Phi_0 \left(\frac{E}{E_\pi^{GC}}\right)^{-\Gamma_1} & \text{if } E_\gamma \leq E_\pi^{GC}, \\ \Phi_0 \left(\frac{E}{E_\pi^{GC}}\right)^{-\Gamma_2} & \text{if } E_\pi^{GC} < E_\gamma < E_\pi^{cut}, \\ \Phi_0 \left(\frac{E}{E_\pi^{GC}}\right)^{-\Gamma_2} \exp\left(-\frac{E}{E_\pi^{cut}} + 1\right), & \text{if } E \geq E_\pi^{cut}, \end{cases} \quad (2.11)$$

where

$$E_\pi^{cut} = \alpha E_\pi^{max}, \quad (2.12)$$

we assume $\alpha = 0.1$ in this work. Note that the energy is the GeV-unit. A schematic GC-spectrum is presented in figure 2.

Although the breaks in spectrum with an exponential cutoff are ubiquitous either for the leptonic or hadronic scenarios, the GC-spectrum (2.11) has its own features. (i) The shape of gamma-ray spectra in leptonic and traditional (without the GC effect)

hadronic models sensitively depend on the distribution of parent particles (electrons or protons), while the GC-spectrum is characterized by a few free parameters ($\Phi_0, \Gamma_1, \Gamma_2, \alpha$ and E_π^{GC}), where the incalculable pp interactions are simplified by the saturation condition in equation (2.3). (ii) On both sides of the sharp breaking point E_π^{GC} the spectrum appears as the single power-law. (iii) The GC-threshold E_π^{GC} in equation (2.10) is nuclear target-dependent, which may be from 100 GeV to TeV and beyond (see discussions in section 5). (iv) Equation (2.10) is an analytical solution of the GC model, where the parameters have their physical meaning and we will use them to predict the undetected spectra in section 4.

3 HESSs J1825-137, J1640-465, J1809-193, J1813-178 and PSR J0205+6449/3C 58

Although a lot of data about the VHE gamma ray spectra of pulsars have been reported, however, leptonic emission scenarios are usually favored over hadronic emission scenarios. Besides, astronomical radiations are complex and different emission mechanisms may exist in a same source simultaneously. We found the following five examples in the existing data showing a complete power-law as shown in figure 2.

HESS J1825-137 is one of the most efficient TeV gamma ray emitting PWNe [9]. It was detected by the Fermi Large Area Telescope(Fermi-LAT) in the GeV energy band, and usually discussed in connection with leptonic acceleration scenarios [10] since it is not a prime candidate for pion decay according to the traditional hadronic scenario. We found that HESS J1825-137 with the Fermi-LAT data in $10 \text{ GeV} - 10 \text{ TeV}$ can also be fitted using the GC-spectrum (see figure 3), where the $E_\pi^{cut} = 14 \text{ TeV}$ is fixed by equation (2.12). For comparison, we present a leptonic spectrum in figure 3 (dashed curve).

HESS J1640-465 is one of the TeV sources discovered by the HESS survey in inner Galaxy [11]. It's spectrum, explained in the traditional hadronic model [12,13], is con-

nected to a hard Fermi-LAT gamma-ray spectrum and it forms a long flat spectrum from 100 MeV to 1 TeV . However, Y.L. Xin et al have suspected that there could not be such a strong proton flux in pulsars [14]. They reanalyzed the relating Fermi-LAT data and found that an extended GeV gamma-ray source was coincident with J1640-465. Its photon spectrum was described by a power-law with an index of 1.42 ± 0.19 in the energy range of 10 – 500 GeV , and smoothly connected with the TeV spectrum of HESS J1640-465. Using the same Fermi-LAT data we describe the expanded spectrum of HESS J1640-465 in the GC model, and the result is presented in figure 4 (solid curve).

HESS J1809-193 was initially discovered during the systematic search for VHE emission from pulsars in the Galactic Plane Survey performed with HESS [15]. The environment of HESS J1809-193 is complicated, containing several different sources. Combining with the Fermi LAT data, the spectrum presents a broad energy plateau in 300 GeV – 30 TeV , the nature of which with such a shape has been regarded as the traditional hadronic model but with a harder proton index. We take an alternate way, i.e, assuming this broadly extended gamma-ray spectrum might be produced by the leptonic radiation and the hadronic model with the GC effect. To begin with, we use the precise data for $dN/dE \sim E^{-\Gamma_2}$ [8] and equation (2.11) to obtain $\Gamma_2 = 2.22$ (see figure 5). Figure 6 is our result using the GC spectrum (2.11), the data are taken from [14].

A high energy pulsar PSR J1813-178 is classified as a PWN candidate, which has a similar spectrum of figure 2. A new detection of extended emission in the range 0.5 – 500 GeV finds that it is difficult to explain the spectrum with inverse Compton (IC) emission from high-energy electrons alone [16]. Our predictions of GC (mixing with leptonic models) are presented in figure 7.

3C 58, classified as a pulsar wind nebula [17], is a complex radio source with an extended flat spectrum. PSR J0205+6449 is a pulsar near 3C 58, it's flux is divided into

two parts: off-peak and on-peak. We connect the off-peak part of PSR J0205+6449 with the flux of 3C 58, the result can be fitted by the GC model as shown in figure 8, and the on-peak part can be described by other leptonic model.

4 HESSs J1826-130, J1641-463 and J1741-302

There are several VHE sources presenting a typical power law with the hard photon index $\Gamma_\gamma \sim 2$ in a broad energy range from hundreds of GeV to beyond 10 TeV. Besides, all of them are tagged as unidentified and located near other bright VHE sources. Although many works have speculated the possible origins of these VHE gamma-ray spectra, their nature is still open. Especially, where and how cosmic rays are accelerated to reach the necessary PeV energies and beyond in our Galaxy, and in which mechanism the kinetic energy of the initial particles (protons or electrons) converts into photons are still unknown. An important obstacle is that we lack the extension of the above spectra in the GeV-energy region, and an incomplete spectrum cannot provide the correct information of these sources. The GC-model predicts the typical broken power law, it reduces the number of free parameters and accordingly the uncertainty. We will use the GC-model to predict the incomplete spectra of the following three examples.

J1826-130 is an unidentified hard spectrum source discovered by HESS along the Galactic plane [18], and was previously hidden in the extended tail of emission from the nearby bright source HESS J1825-137. HESS J1826-130 shows a relatively hard gamma-ray spectrum, which obviously incomplete. However we can perfect it by using the GC model. Our logical reasoning is: (i) Using equation (2.11) at $E_\gamma > E_\pi^{GC}$ to fit the HESS J1826-130 data, one can find that a single power law with $\Gamma_\gamma \sim 2$ extends up to 14 TeV, and then appears a cut-off factor (see figure 9). According to equations (2.9) and (2.12), the breaking energy is $E_\pi^{GC} = 100 \text{ GeV}$. (ii) We turn to HESS J1825-137 for information

related to HESS J1826-130. Note that the parameter β_p in the GC model is determined by the accelerate mechanism of protons. Therefore, we assume that the two sources are close to each other and have a same value β_p . Thus, we have $\Gamma_2 = -\beta_\gamma + 2 \times 0.91 - 1 = 2$ for HESS J1826-130. As a result a complete spectrum of J1826-130 can be shown in figure 10 since we already know $\beta_\gamma = 1.18$.

Why there is no recorded spectrum of HESS J1826-130 at $E_\gamma < 100 \text{ GeV}$? We noticed that a gamma-ray pulsar J1826-1256 was discovered by Fermi-LAT [19], and it's spectrum at the GeV energies is shown in figure 10, which may shadow the spectrum of HESS J1826-130 in the observation and leads to an incomplete spectrum.

A similar example is HESS J1641-463 [20], whose spectrum is also unclear due to the confusion with the bright nearby source HESS J1640-465 [11]. No X -ray candidate stands out as a clear association. Usually it's spectrum is explained by hadronic mechanism, where the emission is produced by cosmic ray protons colliding with the ambient gas [21]. The data in figure 11 tells us that $\Gamma_2 = 2.07$, $E_\pi^{cut} = 14 \text{ TeV}$ in the GC model, and accordingly $E_\pi^{GC} = 0.1 \text{ TeV}$ by equation (2.9). We take $\beta_p = 1.02$ in HESS J1641-463 as in HESS J1640-465 assuming their proton flux are originated from a same accelerator, consequently $\beta_\gamma = 0.99$. Similarly, a complete spectrum of J1641-463 is presented in figure 12. The hollow points are the detected pulsed emission of SNR G338.5+0.1 by Fermi-LAT [22], we add it in figure 12 for they may cover the extension of the HESS spectrum in the GeV energies.

A preliminary detection of HESS J1741-302 was early announced by HESS [23] and thanks to the increased amount of high quality VHE data and improved analysis techniques, the spectrum of it can now be analyzed in detail [21]. HESS J1741-302 is not only unidentified but also has no plausible counterpart at the high-energy ($0.1 \text{ GeV} - 100 \text{ GeV}$) range, the region around it is rather complex, as a compact radio source and a variable star

are spatially coincident with the position of HESS J1741-302. There is only one incomplete spectrum as shown in figure 13, again using the GC model we try to unveil its nature. From the gamma ray distribution in figure 13, one can find that $\beta_\gamma + 2\beta_p - 1 = \Gamma_2 = 2.3$, and $E_\pi^{cut} \simeq 14 \text{ TeV}$ corresponds to $E_\pi^{GC} = 0.1 \text{ TeV}$. Thus, we have got $\beta_p = 0.91$ and 1.02 for J1826-130 and J1641-463, differed by 0.11. Besides, the measured value of Γ_2 for these two sources has an error of 0.11 ± 0.20 . Therefore, we assume that the above three VHE gamma rays originate from the same proton accelerate mechanism in our Galaxy and we take $\beta_p \simeq 1$ for J1741-302. Thus, a complete VHE gamma ray spectrum can be predicted in figure 14. An investigation of Fermi LAT data has revealed a new high energy source Fermi J1740.1-3013 [24], which is $\sim 0.3^\circ$ offset from the best fit position of HESS J1741-302. We presented it in figure 14 considering that the spectrum of HESS J1741-302 at GeV energies may be covered or mixed by this new source.

5 Discussions and Summary

It is generally believed that the gamma rays in pulsar environment are mainly generated by leptonic mechanism since the proton flux is weak. However, with the GC model, the above point of view could be modified. The increment of the pp cross section due to the GC effect may compensate for the lack of proton flux and emit gamma-rays with the GC-characteristics. On the other hand, not all the hadronic accelerators in the Galaxy can generate the GC effect, because comparing with the traditional hadronic model, the GC effect needs higher energy of parent protons to convert into more mesons. Therefore, the hadronic scenario with the GC effect is not as common as leptonic scenario in pulsars.

The inverse Compton emission (or curvature radiation) accompanied by synchrotron X-ray spectrum is an important feature of leptonic model for VHE gamma-ray radiation. The GC model has no such correlation but has a much deeper connection with other

processes. In fact, the GC spectrum (2.11) can be used to explain the VHE gamma ray spectra in supernova remnant (SNR) [5], active galactic nuclei (AGN) [6] and gamma ray burst (GRB) [6]. Besides, adding the process $\gamma \rightarrow e^- + e^+$ or a hadronization mechanism, the same GC model can investigate anomalous excess in electron-positron spectra [5] or hadronic fluxes [7].

A question needs to be explained is that different processes may give different parameters in equation (2.11), which are related to the structure and nature of the source, especially, the important parameter $E_\pi^{GC} \simeq 400 \text{ GeV}$ for Tycho's SNR while $E_\pi^{GC} \simeq 100 \text{ GeV}$ for the sources in this work. Why these E_π^{GC} are different is because that they are target nuclei number A -dependent: $E_\pi^{GC}(p - A) > E_\pi^{GC}(p - A')$ (if $A < A'$) since the nonlinear corrections enhance as A increases. A roughly simulation of the GC model shows that GC-threshold E_π^{GC} drops rapidly from $A = 1$ and then decrease slowly from the intermediate nucleus [3,4]. We divide the targets into a few of categories and assume that on average, target nuclei near pulsar is heavier than that in Tycho's SNR. As discussed above, the broken points E_π^{GC} in the GC model are concentrated around a few different values. A detailed estimation requires more precise examples to be collected. The spectrum of the investigated pulsars is compatible with being produced through the GC effect, compensating for a weak flux of hadrons. Therefore, as shown in figures 4, 6-8, 10, 12 and 14, the GC-spectrum is always accompanied by a leptonic spectrum, although the leptonic fit is beyond the scope of this work. The parameters used/fitted for each source are presented in table 1. An exception in our examples is HESS J1825-137, it extends to a long distance from the central pulsar PSR J1826-1334, where the electrons may escape from the nebula and diffuse in the interstellar medium [25].

In summary, the gluon condensation originating from a nonlinear QCD evolution equation may greatly increase the cross sections of proton-target interactions and arise a char-

acteristic broken power law in the gamma-ray spectra. The result is used to explore the gluon condensation signature in the observed gamma-ray spectra from pulsars.

Acknowledgments: We thank Zhiyi Cui and Lihong Wan for useful comments. This work is supported by the National Natural Science of China (No.11851303).

References

- [1] W. Zhu, Z.Q. Shen and J.H. Ruan, *Can a chaotic solution in the QCD evolution equation restrain high-energy collider physics?* *Chin. Phys. Lett.* **25** (2008) 3605 [arXiv:0809.0609].
- [2] W. Zhu, Z.Q. Shen and J.H. Ruan, *The chaotic effects in a nonlinear QCD evolution equation*, *Nucl. Phys.* **B911** (2016) 1 [arXiv:1603.04158]
- [3] W. Zhu and J. Lan, *The gluon condensation at high energy hadron collisions*, *Nucl. Phys.* **B916** (2017) 647 [arXiv:1702.02249].
- [4] W. Zhu, J.S. Lan and J.H. Ruan, *The gluon condensation in high energy cosmic rays*, *Int. J. Mod. Physics* **E27** (2018) 1850073 [arXiv:1709.03897].
- [5] W. Zhu, P. Liu, J.H. Ruan and F. Wang, *Possible Evidence for the Gluon Condensation Effect in Cosmic Positron and GammaRay Spectra*, *Astrophys. J.* **889** (2020) 127 [arXiv:1912.12842].
- [6] W. Zhu, Z.C. Zheng, P. Liu, L.H. Wan, J.H. Ruan and F. Wang, *Looking for the possible gluon condensation signature in sub-TeV gamma-ray spectra: from active galactic nuclei to gamma ray bursts*, *JCAP* **01** (2021) 038[arXiv:2009.01984].

- [7] W. Zhu, P. Liu, J.H. Ruan, R.Q. Wang and F. Wang, *The gluon condensation effect in the cosmic hadron spectra*, *JCAP* **09** (2020) 011 [arXiv:2002.06294].
- [8] F.A. Aharonian, *Very high energy cosmic gamma radiation: a crucial window on extreme universe*, World Scientific Co. Pte. Ltd. (2004).
- [9] F.A. Aharonian, et al., *A possible association of the new VHE gamma-ray source HESS J1825-137 with the pulsar wind nebula G18.0-0.7*, *A&A* **442** (2005) 25 [arXiv:0519304].
- [10] G. Principe, A.M.W. Mitchell, S. Caroff, J. A. Hinton, R.D. Parsons and S. Funk, *Energy dependent morphology of the pulsar wind nebula HESS J1825-137 with Fermi-LAT*, *A&A* **640** (2020) A76 [arXiv:2006.11177].
- [11] F. Aharonian, A.G. Akhperjanian, A.R. Bazer-Bachi, et al. *The H.E.S.S. survey of the Inner Galaxy in very-high-energy gamma-rays*, *A&A* **636** (2006) 777 [arXiv:0510397].
- [12] M. Lemoine-Goumard, M.-H. Grondin, F. Acero, J. Ballet, H. Laffon, T. Reposeur, *HESS J1640-465 and HESS J1641-463: two intriguing TeV sources in the light of new Fermi LAT observations*, *Astrophys.J.Lett.* **794** (2014) L16 [arXiv:1409.4994].
- [13] L. Supan, A. D. Supanitsky, G. Castelletti, *The environment of the gamma-ray emitting SNR G338.3-0.0: a hadronic interpretation for HESS J1640-465*, *A&A* **589** (2016) A51 [arXiv:1603.05137].
- [14] Y.L. Xin, N.H. Liao, X.L. Guo, Q. Yuan, S.M. Liu¹, Y.Z. Fan and D.M. Wei, *HESS J1640-465-A gamma-ray emitting pulsar wind nebula?* *Astrophys.J.* **867** (2018) 55 [arXiv:1802.03520].

- [15] M. Renaud, S. Hoppe, N. Komin, E. Moulin, V. Marandon and A.C. Clapson, (on behalf of the H.E.S.S. Collaboration) *Pulsar Wind Nebula candidates recently discovered by H.E.S.S.* Proceedings of "4th Heidelberg International Symposium on High Energy Gamma-Ray Astronomy 2008 [arXiv:0811.1559].
- [16] M. Araya, *GeV emission in the region of HESS J1809-193 and HESS J1813-178: Is HESS J1809-193 a proton pevatron?* *Astrophys. J.* **859** (2018) 69 [arXiv:1804.03325].
- [17] J. Li, D. F. Torres, T.T. Lin, M.H Grondin, M. Kerr, M. Lemoine-Goumard, E. de Ona Wilhelmi, *Observing and modeling the gamma-ray emission from pulsar/pulsar wind nebula complex PSR J0205+6449/3C 58.* *Astrophys. J.* **858** (2018) 84 [arXiv:1803.10863].
- [18] E.O. Angner, F. Aharonian, P. Bordas, et al., (H.E.S.S. Collaboration), *HESS J1826-130: A Very Hard γ -Ray Spectrum Source in the Galactic Plane*, *AIP Conf. Proc.*, **1792** (2017) 040024 [arXiv:1701.07002].
- [19] J. Li, D.F. Torres, F. Coti Zelati, A. Papitto, M. Kerr and N. Rea, *Theoretically motivated search and detection of non-thermal pulsations from PSRs J1747-2958, J2021+3651 and J1826-1256*, *Astrophys.J.Lett.* **868** (2018) L29 [arXiv:1811.08339].
- [20] A. Abramowski, F. Aharonian, F. Ait Benkhali, et al. (H.E.S.S. Collaboration), *Discovery of the hard spectrum VHE γ -ray source HESS J1641-463*, *Astrophys. J.* **794** (2014) L1 [arXiv:1408.5280].
- [21] H. Abdalla, A. Abramowski, F. Aharonian et al., *HESS J1741-302: a hidden accelerator in the Galactic plane*, *A&A* **bfA13** (2018) 612 [arXiv:1711.01350].
- [22] M. Lemoine-Goumard, M. H. Grondin, F. Acero, J. Ballet, H. Laffon and T. Reposeur, *HESS J1640-465 and HESS J1641-463: Two intriguing TeV sources*

- in the light of new Fermi TAT observations*, *Astrophys.J.Lett.* **94** (2014) L16 [arXiv:1409.4994].
- [23] O. Tibolla, N. Komin, K. Kosack and M. Naumann-Godo, *High energy gamma-ray astronomy*, *AIP Conf. Proc.*, **1085** (2008) 249.
- [24] C. Y. Hui, P. K. H. Yeung, C. W. Ng, L. C. C. Lin, P. H. T. Tam, K. S. Cheng, A. K. H. Kong, D. O. Chernyshov and V. A. Dogiel, *Observing two dark accelerators around the Galactic Centre with Fermi Large Area Telescope*, *Mon.Not.Roy. Astron.Soc.* **457** (2016) 4262 [arXiv:1601.06500].
- [25] D. Khangulyan, A.V. Koldoba, G. Ustyugova, S.V. Bogovalov, and F. Aharonian, *On the anomalously large extension of the pulsar wind nebula HESS J1825-137*. *Astrophys. J.* **860** (2018) 59 [arXiv:1712.10161].

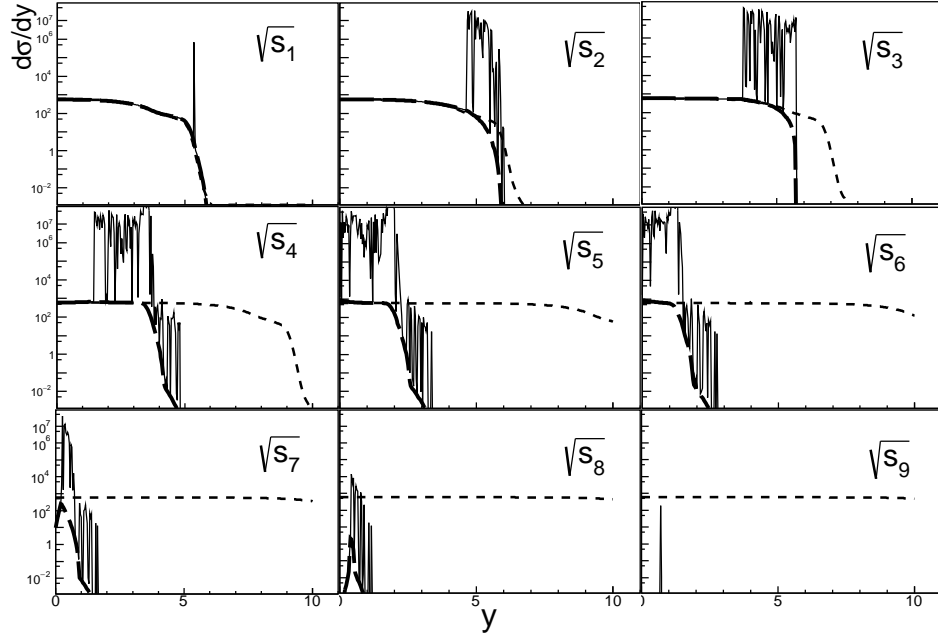


Figure 1: A schematic diagram for the inclusive gluon rapidity distribution at the pp collision [3], where $\sqrt{s_{i+1}} > \sqrt{s_i}$. The results show the large fluctuations arisen by the GC effect.

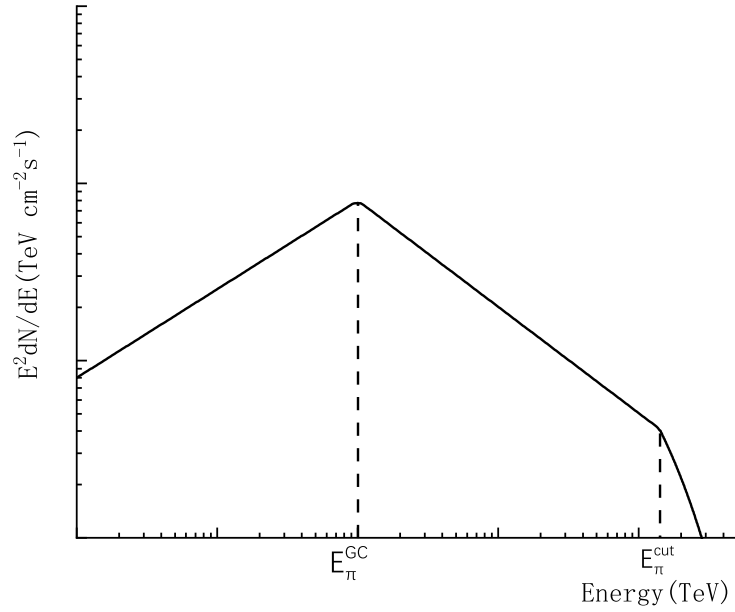


Figure 2: A schematic shape of a complete GC-spectrum according to equation (2.11).

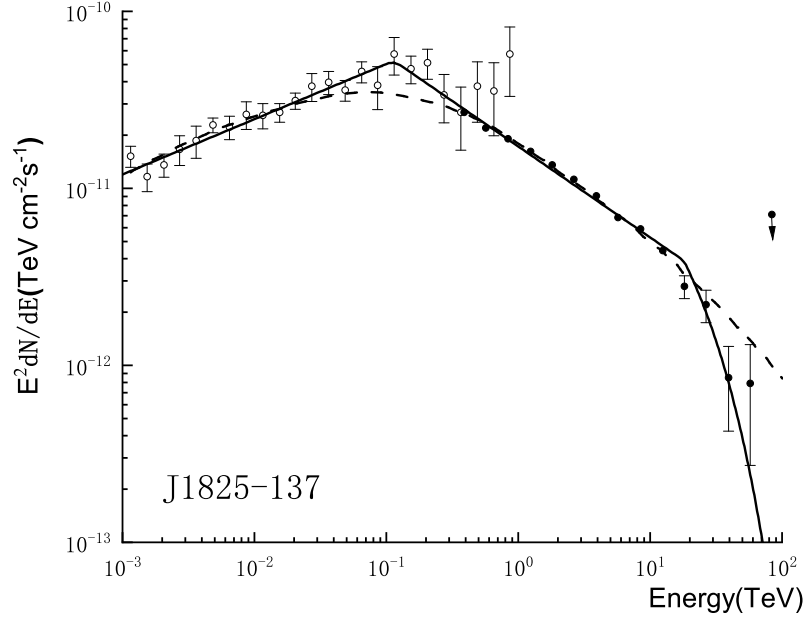


Figure 3: Gamma-ray spectrum of HESS J1825-137 (black points) combined with the Fermi-LAT data (hollow points) [9]. The solid curve is obtained by the GC model, and the dashed curve is the prediction of a leptonic model [10].

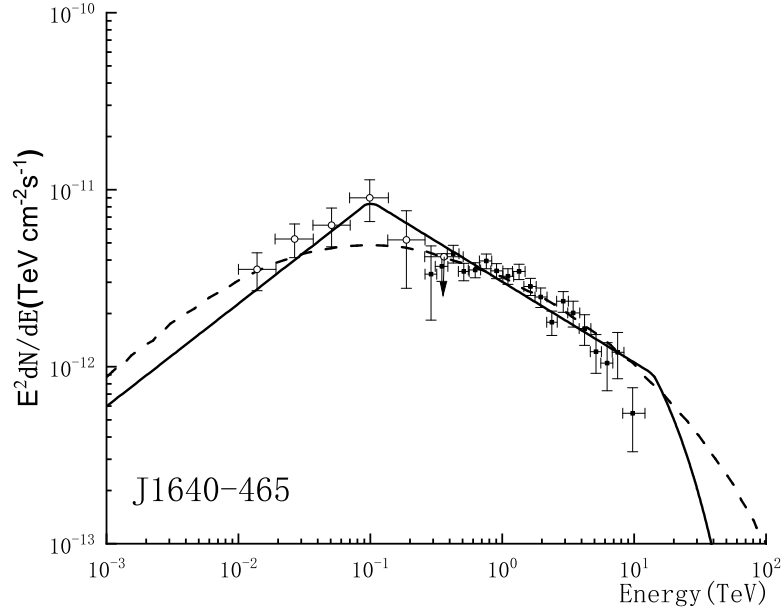


Figure 4: Gamma-ray spectrum of HESS J1640-465 (black points) combined with the Fermi-LAT data (hollow points) [11]. The solid curve is obtained by the GC model. The dashed curve is the prediction of a leptonic model [14].

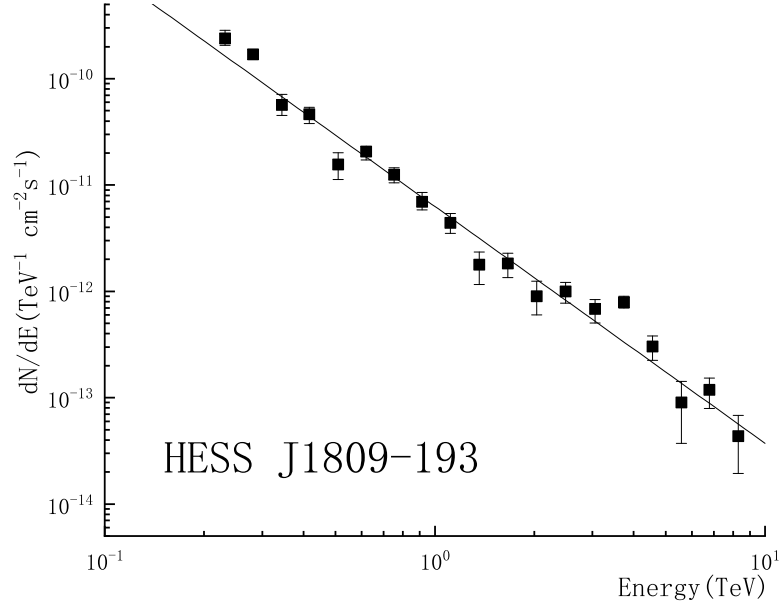


Figure 5: A part of gamma-ray spectrum of HESS J1809-193 [9], which gives $\Gamma_2 = 2.22$.

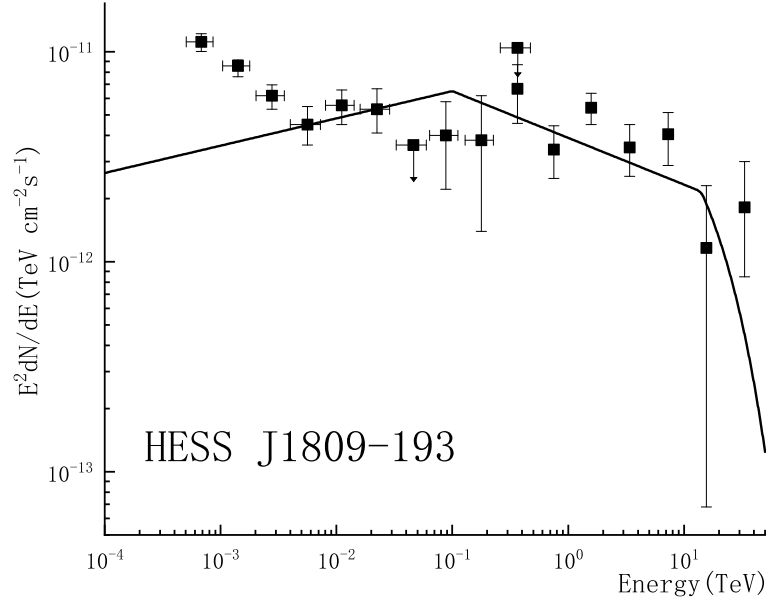


Figure 6: Gamma-ray spectrum of HESS J1809-193 [15]. The solid curve is obtained by the GC model. The experimental points deviated from the GC-spectrum at $E < 10$ GeV may originate from other radiation mechanism.

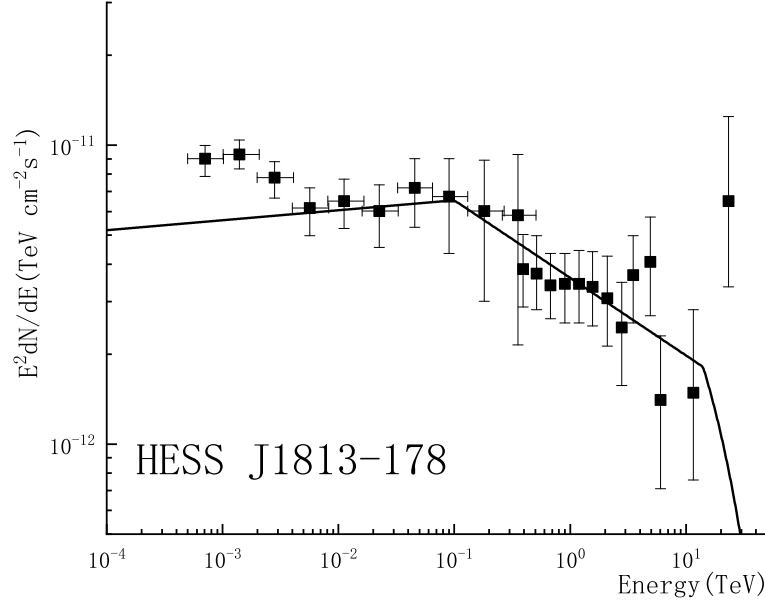


Figure 7: Gamma-ray spectrum of HESS J1813-178 [16]. The solid curve is obtained by the GC model. The experimental points deviated from the GC-spectrum at $E < 10$ GeV may originate from other radiation mechanism.

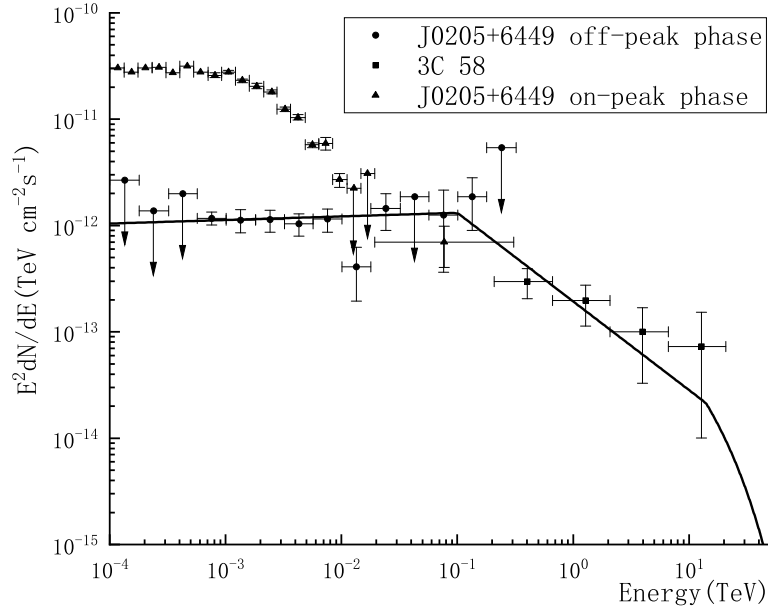


Figure 8: Gamma-ray distribution of 3C 58 combined with off-peak part of PSR J0205+6449 [17]. The solid curve is obtained by the GC model. The on-peak points may originate from other radiation mechanism.

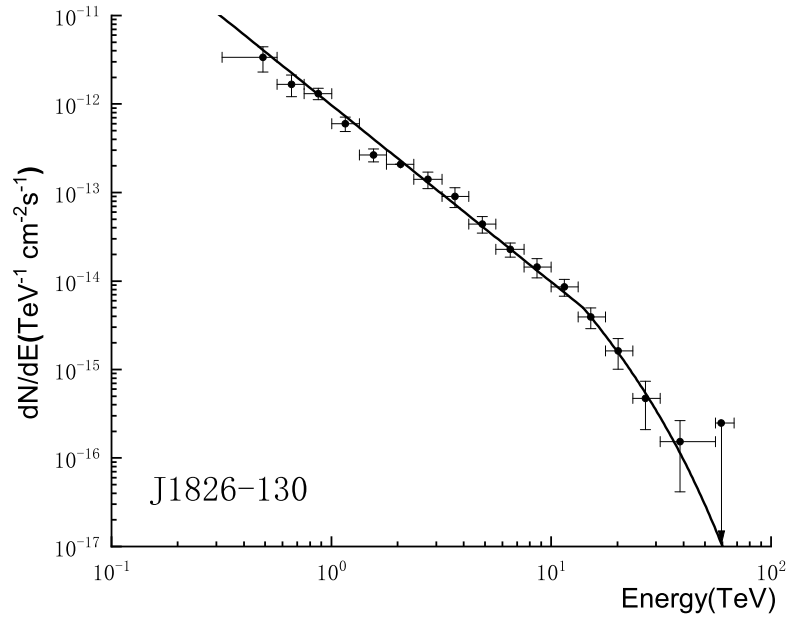


Figure 9: An incomplete gamma-ray spectrum of HESS J1826-130. The data are from HESS [18]. The parameters of the GC model are $\Gamma_2 = 2$ and $E_\pi^{cut} = 18 \text{ TeV}$ in equation (2.11).

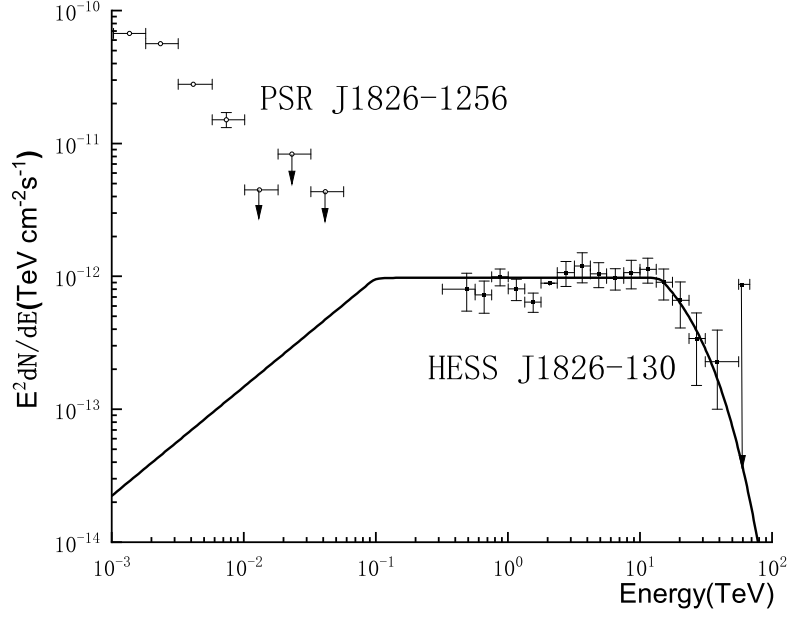


Figure 10: Gamma-ray spectrum of HESS J1826-130 predicted by the GC model (solid curve). The parameter $\beta_p \equiv 0.91$ is fixed by HESS J1640-465. The hollow points are related to a neighboring PSR J1826-1256 [9], which may shadow the spectrum of HESS J1826-130 at $E_\gamma < 0.1$ TeV.

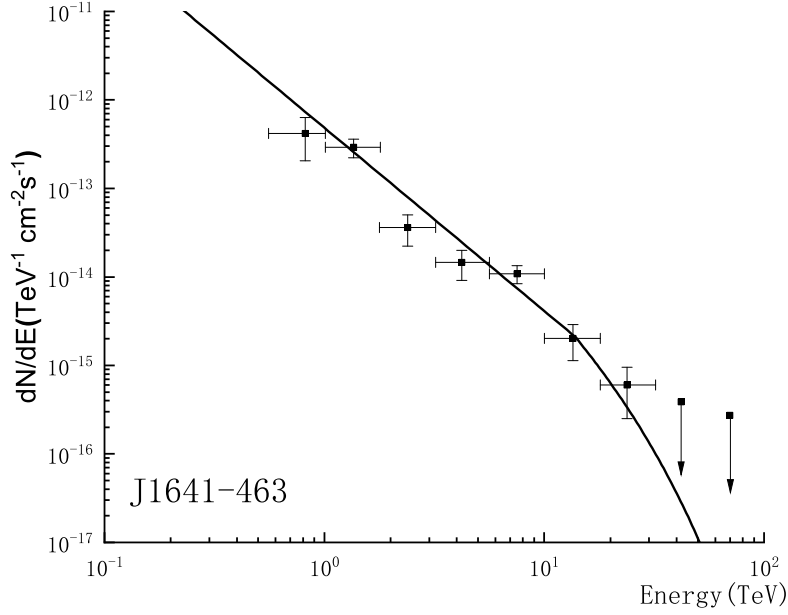


Figure 11: An incomplete gamma-ray spectrum of HESS J1641-463 [20]. The parameters of the GC model are $\Gamma_2 = 2.07$ and $E_\pi^{cut} = 14$ TeV in equation (2.11).

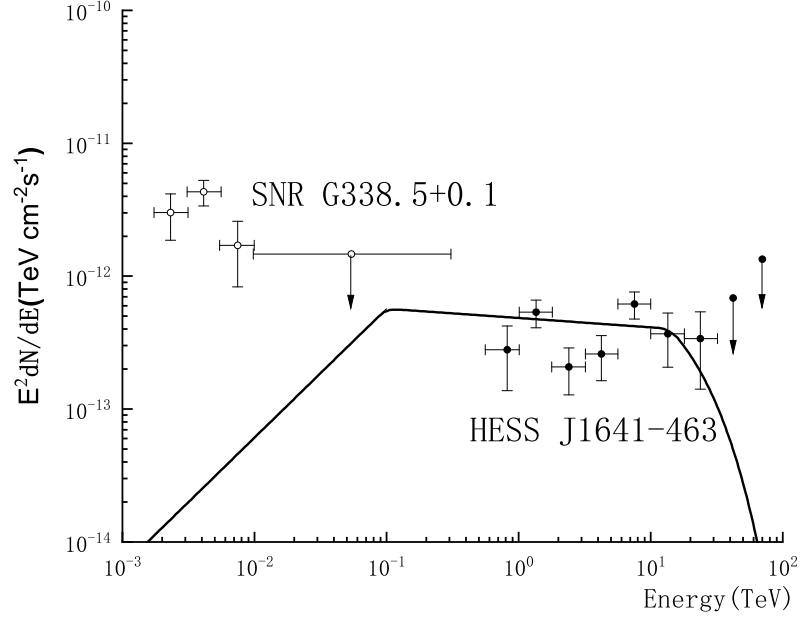


Figure 12: Gamma-ray spectrum of HESS J1641-463 predicted by the GC model (solid curve). The parameter $\beta_p \equiv 1.02$ is fixed by HESS J1640-465. The hollow points are related to a neighboring SNR G338.5+0.1 [14], which may shadow the spectrum of J1641-463 at $E_\gamma < 0.1 \text{ TeV}$.

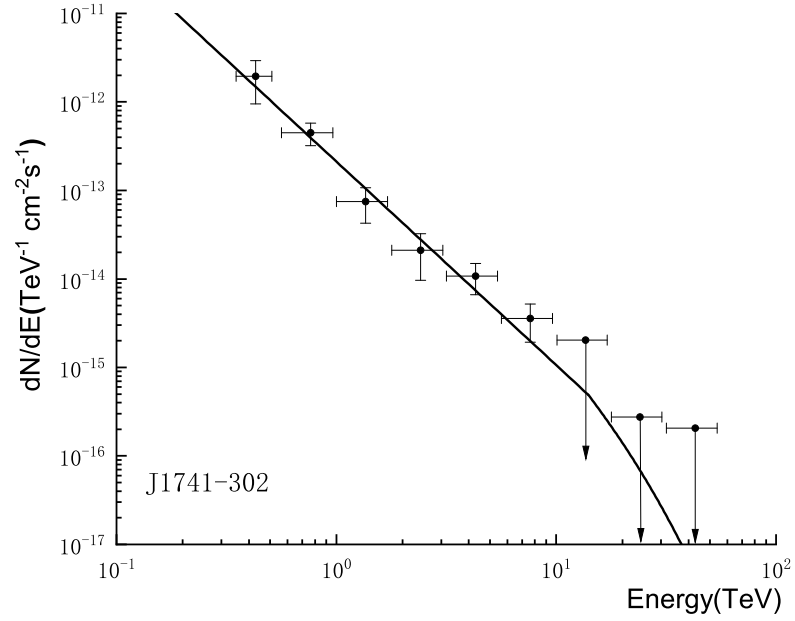


Figure 13: An incomplete gamma-ray spectrum of HESS J1741-302 [21]. The parameters of the GC model are $\Gamma_2 = 2.3$ and $E_\pi^{cut} = 14 \text{ TeV}$ in equation (2.11).

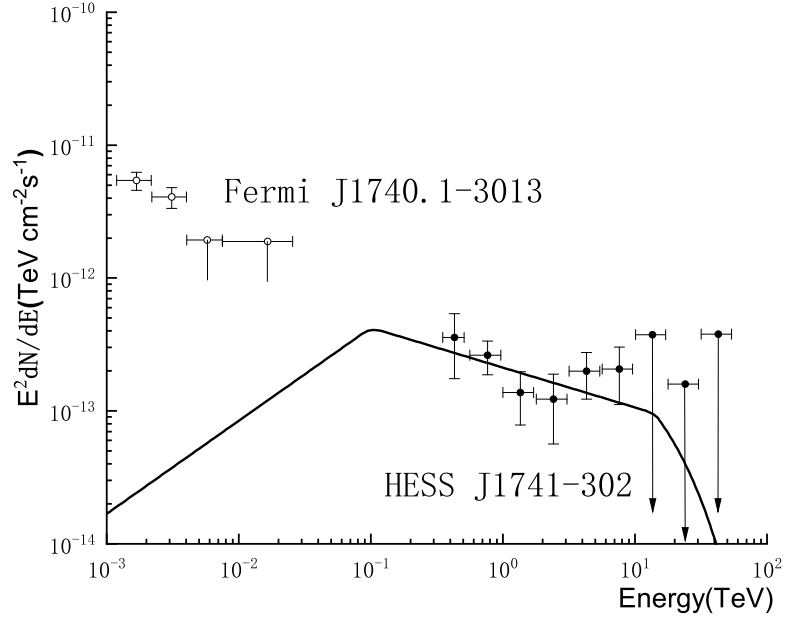


Figure 14: Gamma-ray spectrum of HESS J1741-302 predicted by the GC model (solid curve). The parameter $\beta_p \equiv 1$ refers to HESS J1641-463 and HESS J1826-139. The hollow points are related to a neighboring Fermi J1740.1-3013 [24], which may shadow the spectrum of J1741-302 at $E_\gamma < 0.1 \text{ TeV}$.

Table 1: Parameters of γ -ray spectra of pulsars in the GC-model.

1

TABLE I.

Name	$\Phi_0(TeV^{-1}cm^{-2}s^{-1})$	Γ_1	Γ_2	$E_{\pi}^{GC}(TeV)$
J1825-137	4.17×10^{-9}	1.69	2.51	0.11
J1640-465	8.63×10^{-10}	1.42	2.46	0.1
J1809-193	6.5×10^{-10}	1.87	2.22	0.1
J1813-178	6.54×10^{-10}	1.97	2.26	0.1
J1826-130	9.75×10^{-11}	1.18	2	0.1
J1641-463	5.69×10^{-11}	1.03	2.07	0.1
J1741-302	4.23×10^{-11}	1.3	2.3	0.1
3C58	1.32×10^{-10}	1.97	2.83	0.1